



FINAL REPORT

Deep Roots of Geothermal Systems Part 2: Numerical Modelling

Project ID: 13-05-004

Coordinator: Guðni Axelsson/Robert Podgorney

Start date: 01.07.2013

Duration: 3 years

Partners: Iceland GeoSurvey, Verkfræðistofan Vatnaskil, Landsvirkjun, Orkuveita Reykjavíkur, Háskóli Íslands, HS Orka, Orkustofnun, Idaho National Laboratory (USA)

1 Project summary

Work on Part 2 of the DRG (Deep Roots of Geothermal systems) project started in the fall of 2013. This part of the project focuses on application and further development of numerical modelling software that can model volcanic geothermal systems, from the deep magmatic heat sources up to the hydrostatic geothermal system above. The project was split up in two parts (as described in the grant submission document). Part 2.1 was assigned to geothermal reservoir modelling specialists at Iceland GeoSurvey (ÍSOR) and Vatnaskil Consulting Engineers. Part 2.2 was assigned to Lilja Magnúsdóttir, a postdoctoral scholar focusing on geothermal reservoir engineering. Both projects did progress more-or-less according to schedule, although details of the respective schedules underwent some changes in view of the findings of the group. The final third part of the project lasted considerably longer than originally planned, as it is now coming to an end in late 2017, almost a year later than planned. The effort put into the project during this last one-third part was, however, comparable to what was planned originally.

The first annual report for part 2 of the DRG project, which covered the progress up to 1.7.2014, was published in late 2014. The second annual report covered the progress up to late 2015. This final report describes the progress and results of the whole project, but with emphasis on the outcome of the second and third parts of the project.

1.1 Project progress

1.1.1 Progress of Part 2.1

This part of the project was undertaken by Gunnar Þorgilsson at ÍSOR and Jean-Claude Berthet at Vatnaskil, coordinated by Egill Júlíusson at Landsvirkjun, with support from Gudni Axelsson at ÍSOR. This subpart of the project was initially devoted to the Hydrotherm and CSMP++ reservoir modelling software, but later the emphasis shifted to the use of the iTOUGH2 software with the additions developed under part 2.2 of the DERG-project (see later).

Preparatory work was carried out during the fall of 2013 while in January 2014 the two modelling experts went for a two-week visit to ETH in Zurich under the guidance of Dr. Thomas Driesner.

In the months following the visit, Gunnar and Jean-Claude worked on improving their skills with CSMP++ modelling. By the autumn of 2014 they were able to create, run and analyse a simple but realistic 2D model of a reservoir system containing a magma intrusions, as well as having learned to use the 3D capabilities of Hydrotherm.

CSMP++ is not per se a program but rather a library proposing tools to model heat and mass flow, out of which programs are constructed. When the DRG project began, CSMP++ was already well developed. Most of the features needed to model magma intrusions were already implemented. The library had a supercritical equation of state module and tools to model temperature dependent permeabilities. Gunnar and Jean-Claude did some work to create new permeability versus temperature functions. Some work was needed to set up projects and build the programs, but overall the numerical work did not required as much time as originally planned. So the modelling and case study part of the project began soon after Gunnar's and Jean-Claude's visit to ETH in January 2014.

Therefore, The case study and modelling part of the project went further than anticipated (see some results below).

In early 2015, Vatnaskil was granted a testing license for the new iTOUGH2 with the super-critical module implemented by Lilja Magnúsdóttir (part 2.2, see later). Jean-Claude spent some time testing the program and on running models similar to those previously run with HYDROTHERM and CSMP++. Later in the project Gunnar also did some case-study modelling with the updated iTOUGH2-code.

The remainder of subchapter 1.1.1 presents some (5) examples of modelling case studies carried out by the two modelling experts, both purely theoretical as well as linked with real geothermal situations (Krafla and IDDP-1).

1.1.1.1 IDDP-1 case study and CSMP++ modelling

1.1.1.1.1 Concepts and data

Most of the modelling in this case study revolved around the deep well (IDDP1) in Krafla, which drilled into magma. The first step was to gather data and information about the well and the surrounding rock.

The original plan of the Deep Root Project was to drill down to 4.5 km, to find super critical water; as the magma was thought to be below 5 km. But the drilling of the well was stopped at 2.1 km because of magma. Two attempts were made to redirect the well and drill around the magma, but all ended up at around 2.1 km (Pálsson et al., 2014). It is not known how wide the magma intrusion is, and whether it should be described as an intrusion or a larger magma chamber. The first models created were based on the stratigraphy description by Mortensen et al. (2014):

“The upper 1362 m of the well consist of basaltic lavas and hyaloclastite formations [...]”

“Below 1350 m depth IDDP-1 the well enters a dyke complex which extends to the bottom of the well at 2104 m depth, where the well encountered rhyolitic magma.”

“The upper reservoir is isothermal at 170°C.”

“The largest feed-zones [...] were encountered below 2000 m depth [...]”

“[...] in the upper 1300 m of well IDDP1 few smaller feed zones were intersected [...]”

“[...] feed zones are scarce at 1350–2000 m depth. [...] this interval may be characterized as representing a tight cap rock to the lower reservoir.”

1.1.1.1.2 Model based on stratigraphy description

The first step was to test the hypotheses presented in the stratigraphy article (Mortensen et al., 2014). A model was constructed based on the description given in the article (**Figure 1**). The model is 5 km deep and 10 km wide. The model is divided into layers: an upper layer (from the surface down to 1 350 m), a cap rock layer (from 1 350 m down to 2 000 m), a feed-zone layer (2 km to 2.1 km), and a deep layer (below 2.1 km). In the upper layer, where the temperature is uniform at 170 °C, a permeability of 10^{-15} m² was assigned. This permeability was chosen so as to create strong convection in the layer. Below 1350 m, temperature dependent permeabilities were used. The permeability functions, for each layer, are shown in **Figure 2**. For the ductile part (above 400 °C), the

three functions share the same properties. In the brittle region (below 400 °C), the functions were defined so as to reflect the layers' characteristics as described in the stratigraphy article. The caprock layer was assigned a low brittle permeability of 10^{-17} m^2 , so as to create a tight caprock. The feedzone layer was assigned the brittle permeability of 10^{-14} m^2 ; and the deep layer was assigned a brittle permeability of 10^{-15} m^2 . The top boundary was set to a constant temperature of 20°C (constant during the simulation); and the bottom was assigned heat sources averaging to a heat flux of 260 mW m^{-2} . The heat flux was chosen so as to obtain, 5 km down, a temperature of 600 °C. The magma intrusion, at the center, is 200 m wide and 3 km high. Its initial temperature was set to 900 °C. Because the permeability is temperature dependent, the intrusion is automatically assigned a low initial permeability of 10^{-22} m^2 .

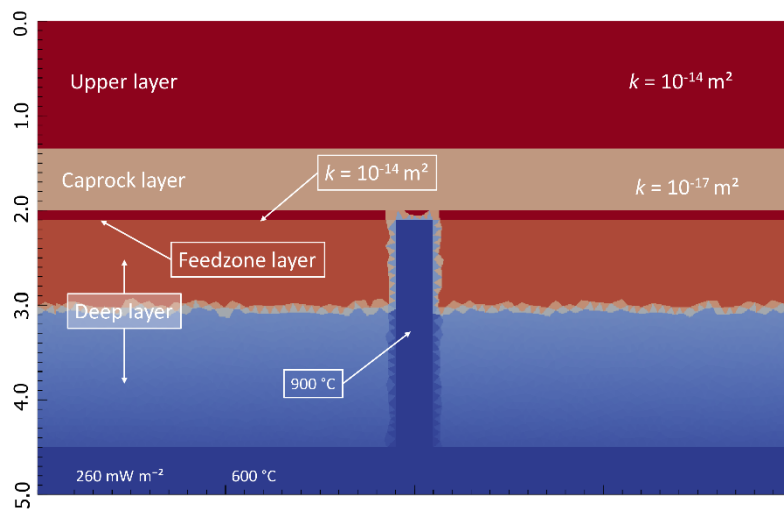


Figure 1. CSMP++ model for IDDP-1 based on the IDDP-1 description by (Mortensen et al., 2014). The figure shows the permeability and temperature in the initial state.

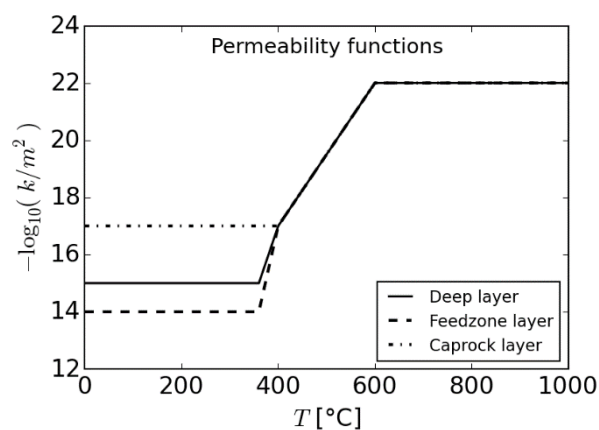


Figure 2. Temperature dependent permeability functions used for the three layers below 1350 m.

CSMP was first used to create a background steady state without the pluton. Then the model was run, with the pluton, to simulate thousands of years. At the beginning of the run, the temperature, above the pluton, is that of the background heat flux (**Figure 3**); the gradient is 0.12 °C/ m. During the first 2 000 years, the heat from the pluton gradually penetrates into the caprock; little change is observed in the upper layer. After around 2 000 years, the heat has crossed the caprock and the temperature in the upper layer begins to rise. After 3 000 years, convection is visible only at the

bottom of the upper layer. After 4 000, the convection has reached the top of the reservoir; the temperature in the upper layer is almost uniform, around 200 °C. During the next 1 000 years, the temperature rises slightly at the top of the upper layer, but overall it changes little.

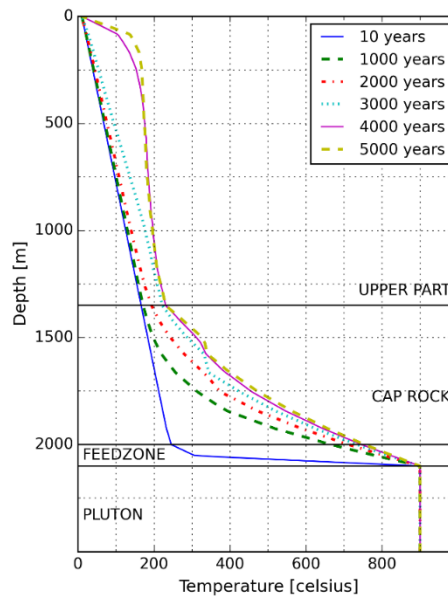


Figure 3. Temperature versus depth at the center of the model, in and above the pluton.

The model manages to reproduce the uniform temperature measured in the upper reservoir. However, the measured temperatures in the supposed caprock, are that of saturated water, whereas the model predicts higher, steam or supercritical temperatures. It is therefore likely that the permeability in the caprock is in reality higher, and that the layer is not as tight as it was assumed to be.

1.1.1.2 Dynamic modeling of a Krafla-like system with CSMP++

One of the possible conceptual models of the Krafla system is that at some point the permeability increased in the upper part Wei15. Here we explore how the natural state of a Krafla-like system could have evolved dynamically with a two-dimensional CSMP++ model. Models of dynamic high temperature geothermal system with sudden changes are usually rather unstable. So in order to make complete runs the finite element mesh was made coarse and the background permeability somewhat lower ($k = 3 \times 10^{-16} \text{ m}^2$) than what is thought to occur in the Krafla system Wei15. These changes help average out sudden changes in temperature and pressure and slows down the evolution of the system. The permeability is made temperature dependent as can be seen in **Figure 4**. There we see that the permeability drops by an order of magnitude on the temperature interval from 100 °C to 200 °C. This drop will crudely model the formation of a dynamic cap-rock due to clay alteration. Also, brittle-ductile transition is set to occur between 600 °C and 700 °C. This is in the lower end where the brittle-ductile transition is thought to happen, Vio10.

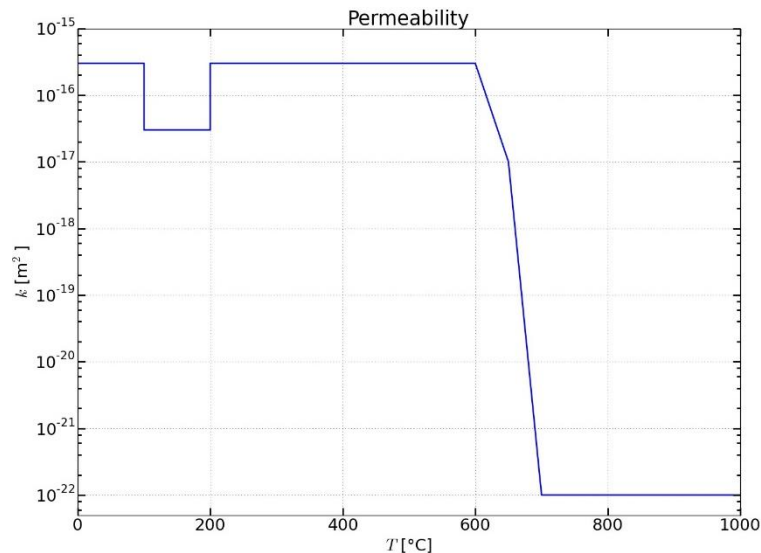


Figure 4. Permeability as a function of temperature. Between 100 °C and 200 °C we have a sudden drop to simulate the formation of cap-rock due to clay-alteration. The brittle-ductile transition is set at the temperature interval from 600 °C to 700 °C.

Figure 5 shows the permeability of the system at various times. Also plotted in **Figure 5**, are temperature contour lines and fluid velocity vectors. The temperature at the contour lines start at 50 °C for the uppermost line and increment by 50 °C downward between lines. The model was made to be 10 km wide and 5 km deep. The top of the model is put at 500 m above sea-level (m.a.s.l.) and the bottom at 4500 m below sea-level (m.b.s.l.). The upper part of the system starts at 200 m.a.s.l. and goes down to 1500 m.b.s.l., see **Figure 5** (a). The initial temperature profile is a linear 100 °C/km gradient. At the bottom we maintain a 210 W m⁻² heat flux throughout the simulation.

After 100 years a 900 °C pluton is injected into the system. The pluton comes in as a 100 m wide and 2 km high column. **Figure 5** (b) shows the system after 200 years. There we see that the pluton is starting to heat up its surroundings.

As time progressed further the heat from the pluton starts a large convection cell at the center and drives the cap-rock up into a dome like structure, see **Figure 5** (c). Also, we see formation of smaller convection cells to sides as time progresses. These convection cells tend to be rather stable as the cap-rock acts as “blanket” over the system and the flow is maintained by the heat-flux from below. The formation of the dome in the cap-rock also helps stabilizing the system by pinning down the large convection cell at the center.

After 6000 years we abruptly lower the background permeability in the upper system. The temperature dependence of the permeability remains similar to what is shown in **Figure 4**. With the increased permeability a new pair of small convection cells form in the upper layer and the cap-rock dome deforms into a more box-like shape. These new arrangement of convection cells also seems to be robust and maintains its structure for at least another 6000 years, see **Figure 5** (d). We can therefore assume that the system shown at **Figure 5** (d) can be regarded as a natural steady state.

The change in the temperature profile of the system caused by the sudden increase of permeability of the upper system can be seen in **Figure 6**. Temperature profiles at various distances from center are plotted just before the change and 2000 year after the change. We see in **Figure 5** (b) that the

temperature profile 300 m from the center has developed a steep curve in the upper level and even a slight temperature inversion 600 m from the center, see **Figure 5 (c)**.

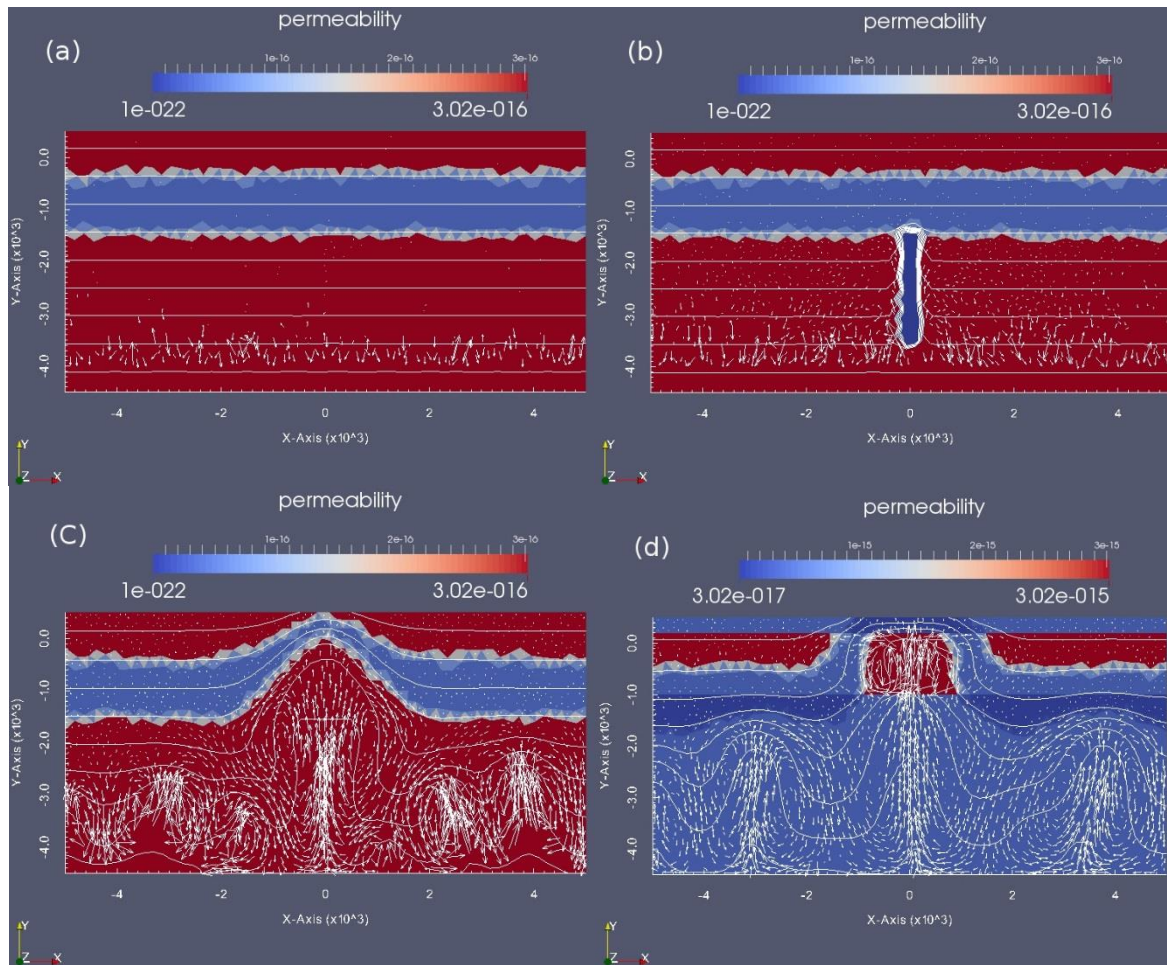


Figure 5. Snapshots of the system at various times. The color indicates the permeability. The white contour lines give the temperature starting from 50 °C at the uppermost line and increasing by 50 °C between lines. Fluid velocity is given by the white arrows. In (a) we see the system after 100 years or just before the pluton injection. Figure (b) shows the system at 200 years, which is shortly after the injection. The heat from the pluton starts a system of convection cells that drives up the cap-Rock. This can be seen in (c) which shows the system after 6000 years. After 6000 years the permeability of the upper system is abruptly increased by an order of magnitude. This forms new convection cells in the upper system. This system is also rather stable as can be seen in (d) which shows the system after 12000 years (Note the change of the color scale).

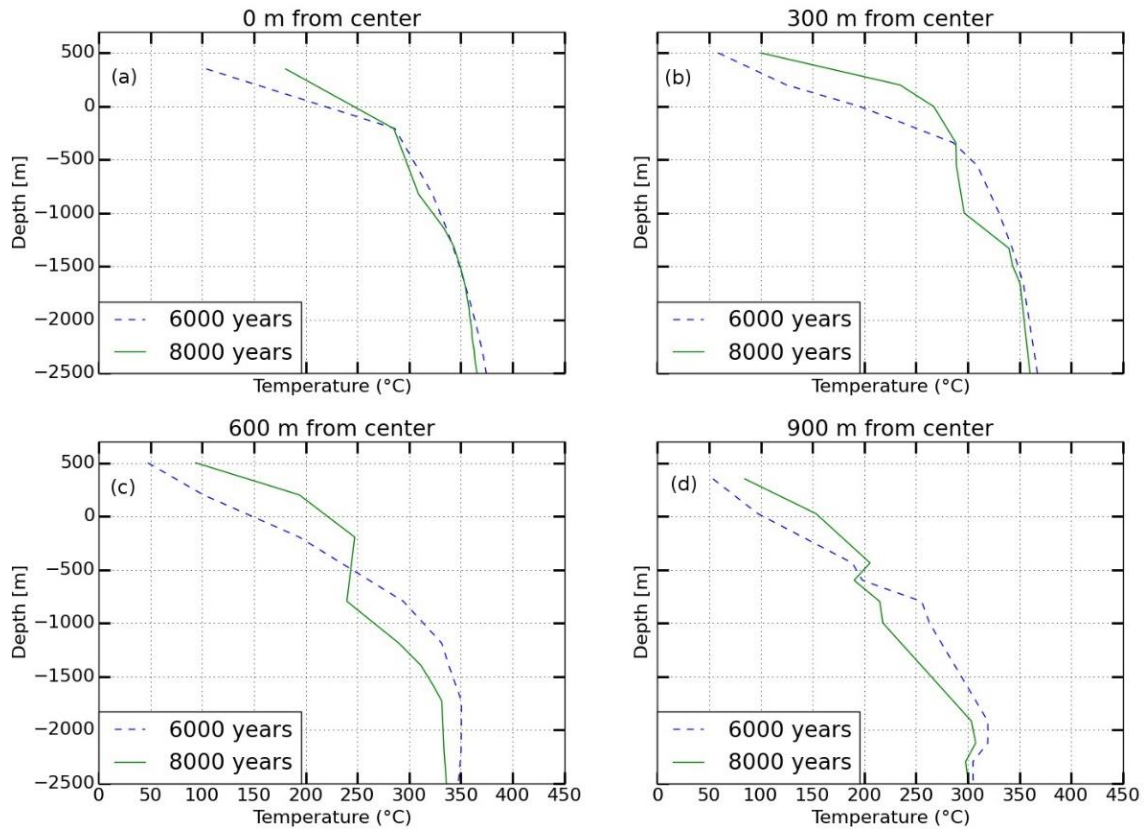


Figure 6. Temperature profiles of the system just before the increase of permeability of the upper system (blue dashed lines) and 2000 years after the increase (green solid lines). Figure (a) shows the profile at the center, (b) 300 m from the center, (c) 600 m from the center, and (d) 900 m from the center.

1.1.1.3 iTOUGH2 models

The first objective of this case study was to try to reproduce the results obtained using HYDROTHERM (Weisenberg, et al., 2015 pp. 61-63) and CSMP++ (*Dynamic modeling of a Krafla-like system with CSMP++*). Models were created with the same characteristics. The models are 3 km deep and include a pluton in the left bottom corner. The pluton is 400 m wide and extends from the bottom up to -2 km (Figure 7). The plutons are introduced in the simulation at a time referred as time zero and have an initial temperature of 750 °C. Prior to the introduction of the plutons, the models are in a steady state and have a steady basalt heat flux of 44 mW m⁻². The basalt heat flux creates a vertical temperature gradient of around 20 °C/km. In CSMP++ and HYDROTHERM, temperature dependent permeabilities were used to simulate the brittle-ductile transition. When this work was performed, this feature had not yet been implemented in iTOUGH2 (version 6.9 beta). Constant permeabilities were used instead. The permeability outside the pluton and below -1 km was set to 10⁻¹⁵ m². Above -1 km, it was set to 50×10⁻¹⁵ m². Inside the pluton the permeability was set to 10⁻²⁰ m². Several models were constructed with different types of mesh.

1.1.1.3.1 Fine mesh model

The model with finest mesh has a node to node distance of 20 m, above and around the pluton (Figure 7). With this mesh, the temperature becomes nearly uniform in the upper reservoir, around 2500 years after the introduction of the pluton (Figure 8). However, the temperatures is uniform only close to the left boundary (10 m and 30 m). Not so far, 50 m and 70 m away, the temperature

gradient is inverted. In a model, a no-flow boundary acts as a plane of symmetry. It is therefore possible from this half model to infer what would be the result for a model twice as long with an 800 m wide pluton at the center. Straight, above the 800 m wide pluton, the temperature would be uniform within a 60 m to 100 m wide region and beyond the temperatures should be inverted. In Krafla, only two wells inside the main production area (Leirbotnar, Suðurhlíðar, Vesturhlíðar and Vítismór) have inverted formation temperatures (K-16 and K-17) even though the main production area is around 2 km wide (**Figure 9**).

Running the models with fine grids was sometimes difficult. The time step often shrank to less than a day thus making the modeling of thousands of years difficult. It is not clear why, or when, such problem occurs, but it seems that this was due to the formation of small convection cells which required small time steps to be modeled.

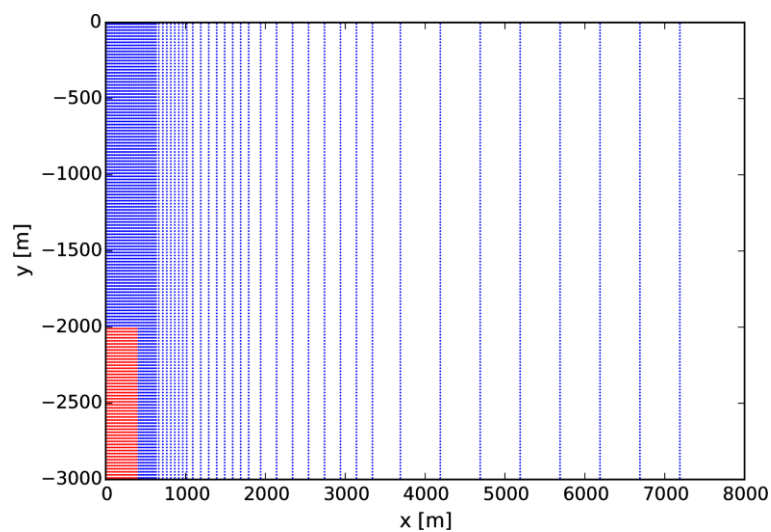


Figure 7. The red and blues dots indicate the locations of the nodes. The red nodes indicates the location of the plutons. The distance between nodes is twenty meters in the convective region (around and above the pluton). Away from the pluton the mesh is coarser.

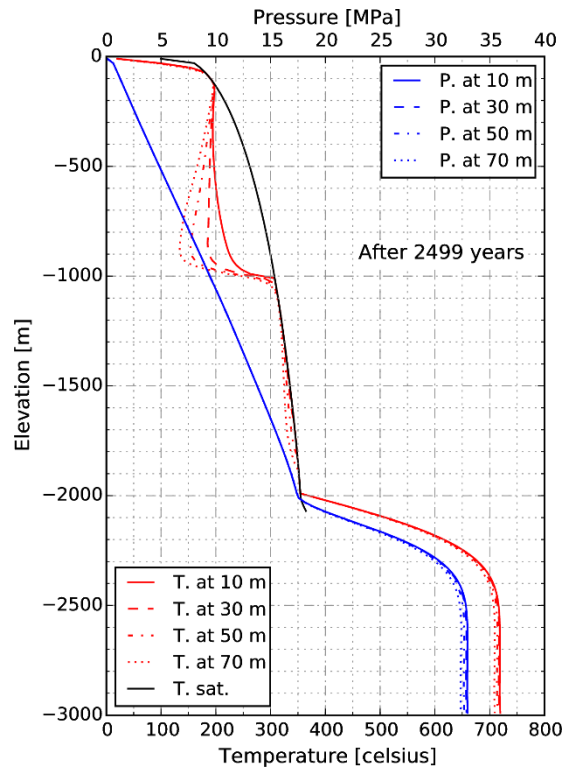


Figure 8. Temperature and pressure (10, 30, 50 and 70) m away from the left boundary, after 2499 years. Results obtained using the fine mesh (20 m between nodes).

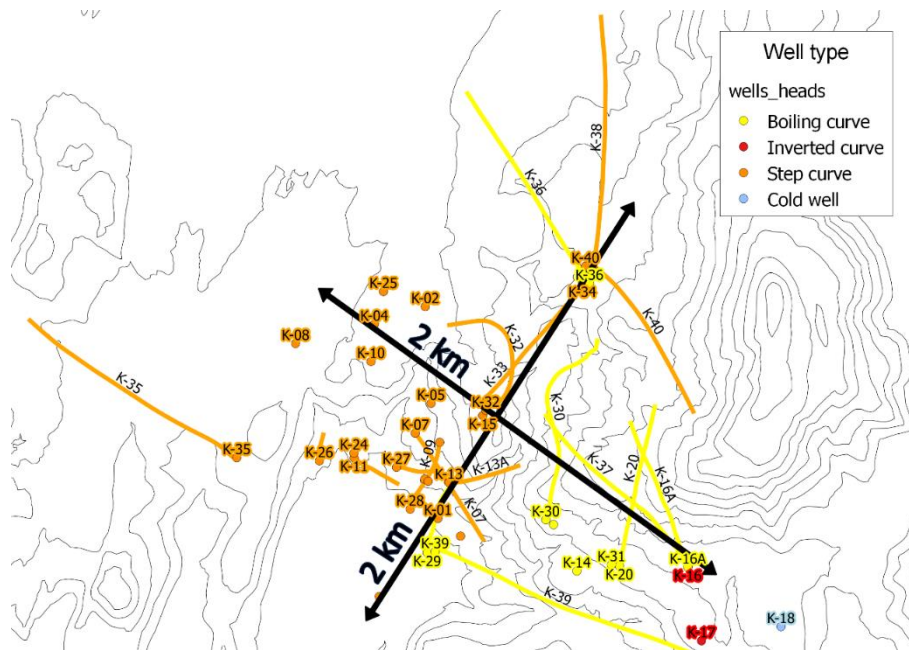


Figure 9. The Krafla main production zone is roughly 2 km wide. The wells are shown in colors that depend on the types of their formation temperature profiles. The wells that have boiling temperature up to the surface are in yellow. The wells that have a sudden temperature drop and an isothermal section are in orange. The wells that have inverted temperatures are in red.

1.1.1.3.2 Comparing meshes

Different mesh densities were tested. Unexpectedly, models with coarser grids run faster, but with coarser grids, the convective fluxes are not model as accurately. **Figure 10** compares the temperature

profiles obtained with different mesh densities: 20 m, 60 m and 180 m between nodes. The figure shows that with the coarsest mesh (180 m), convective fluxes are not sufficiently well modeled. After 2 500 years the upper reservoir is still cold (below 100 °C). Eventually, the upper reservoir heats up, but the stage where upper reservoir is uniformly hot and the lower reservoir on the saturation curve, never happens.

Running tests showed a mesh with a node to node distance of roughly 100 m is the best. The mesh is dense enough to model convection fairly accurately, and the step size does not shrink too much or for too long so as to make a large model impossible to run. In a paper published recently (Scott et al., 2015), Samuel Scott used 10 000 triangular elements for a domain of 5×15 km². This corresponds to a mean node-to-node distance of 87 m. In an earlier paper (Weis et al., 2014), Philipp Weis used 2 790 elements for a domain of 10×3 km²; the mean node-to-node distance is 104 m.

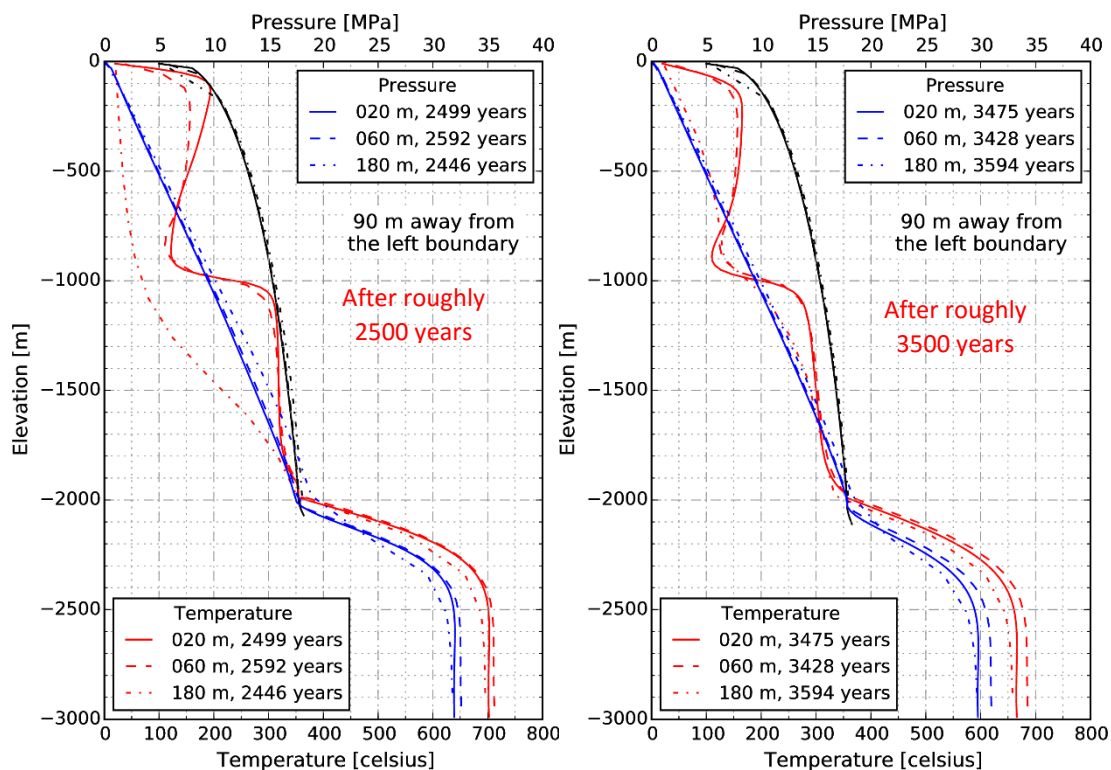


Figure 10. Temperature and pressure 90 m away from the left boundary, after about 2500 years and 3500 years, using different mesh densities (20 m, 60 m and 180 m between nodes).

1.1.1.4 References

Mortensen et al. 2014. Stratigraphy, alteration mineralogy, permeability and temperature conditions of well IDDP-1, Krafla, NE-Iceland. *Geothermics*. 2014, Vol. 49, pp. 31-41.

Pálsson et al. 2014. Drilling of the well IDDP-1. *Geothermics*. 2014, Vol. 49, pp. 23-30.

Scott et al. 2015. Geologic controls on supercritical geothermal resources above magmatic intrusions. *Nature Communications*. 27 July 2015, Vol. 6, 7837.

Weis et al. 2014. Hydrothermal, multiphase convection of H₂O-NaCl fluids from ambient to magmatic temperatures: a new numerical scheme and benchmarks for code comparison. 2014, Vol. 14, 3, pp. 347-371.

Weisenberg et al. 2015. *Revision of the Conceptual Model of the Krafla Geothermal System*. Reykjavik : Landsvirkjun, ÍSOR, Vatnaskil, 2015. LV-2015-040, ISOR-2015/012, Vatnaskil 15.03.

1.1.1.5 Comparison of a dike-like and a pillar-like pluton intrusions in three dimensions using iTOUGH2

This section presents a comparison of three different shapes of shallow pluton intrusions: A pillar-like intrusion, a narrow and long dike-like intrusion, and limited dike-like intrusion. We use iTOUGH2 with the EOS1sc module for the modeling. Here we are not modeling a specific geothermal site but making a more of a general toy-model. For some of the parameters, such as the permeability, the values were chosen to avoid crashes in the simulations.

1.1.1.5.1 Model setup

The system is three dimensional with equal side lengths of $L=2500$ m. It is partitioned into cubes that are connected in a square grid scheme. Nearly all the cubes have a side length $dL = 100$ m except at the top where the cubes are given disproportionately large volume to act as a boundary condition with a constant temperature of 20°C and a pressure of 1 atm. The temperature and pressure at the bottom is also fixed by giving the cubes at the bottom a disproportionately large heat capacity and a zero permeability. The sides of the system have a no flow boundary condition.

The background rock has initially a temperature gradient of $100^{\circ}\text{C}/\text{km}$, a hydrostatic pressure gradient, 10% porosity, specific heat of $900 \text{ J}/(\text{kg } ^{\circ}\text{C})$, density of $2600 \text{ kg}/\text{m}^3$, and a permeability of $5.0 \times 10^{-16} \text{ m}^2 = 0.5 \text{ mD}$.

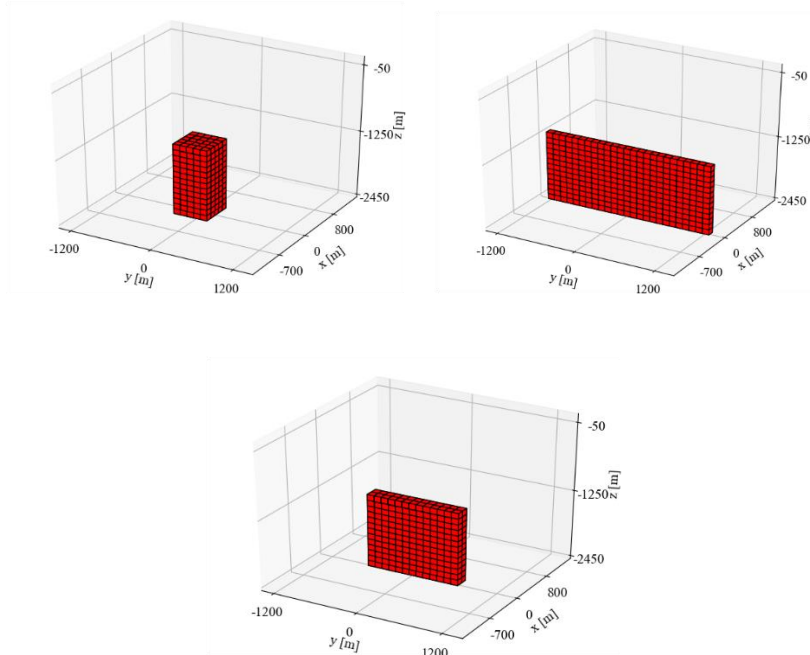


Figure 11. The three shapes of pluton intrusions being compared: (Upper left) a pillar-like intrusion, (upper right) a dike-like intrusion, and (bottom) a limited dike-like intrusion. Both the upper intrusions have the same volume while the limited dike intrusion has a slightly more volume (circa. 4% more).

The intrusions all have nearly the same volume and have the geometrical dimension shown in Figure 11 and Table 1. The long dike intrusion stretches over the whole system, side to side, and acts as a semi two dimensional system.

Table 1. Dimensions of the pluton intrusions

	Height [m]	Width [m]	Length [m]	Number of cubes	Total Volume [m ³]
Pillar intrusion	1300	500	500	325	3.25×10^8
Dike intrusion	1300	100	2500	325	3.25×10^8
Limited dike intrusion	1300	200	1300	338	3.38×10^8

At the beginning all the intrusions have the same temperature of 900 °C, and twice the hydrostatic pressure. In all other respect the intrusions share the same physical features as the background rock.

In both the background rock and the pluton intrusions, the permeability and specific heat is temperature dependent. The value of the permeability decreases log-linearly nine orders of magnitude between the temperatures 600 °C and 700 °C. This is to roughly simulate the ductile-brittle transition. The specific heat increases linearly by a factor of 2 from 750 °C to 800 °C in order to crudely account for the latent heat of the pluton.

At the writing of this report the temperature depended features for permeability and specific heat are not described in the iTOUGH2 manual but can be found in the *i2f.f* file in the source code.

1.1.1.5.2 Simulation results

Figure 12 shows a 3D contour plot along with vector showing the total rate of fluid flow in each element after 200 years. We notice, as expected, that the dike intrusions have cooled more than the pillar intrusion due to higher surface to volume ratio. But we also notice that due to inflow of cold water from the surrounding at the bottom that the heat of the intrusions are being eroded away at the bottom.

As the simulations progresses, the three systems evolve in different ways. After 5000 years the temperature plumes have taken on a semi stable forms that are characteristic for each intrusion. In Figures 3 to 5 cross sections of the systems are shown in the xz-plane cutting the middle of the y-axis. Also in the figures are shown temperature profiles at three different locations in the cross sections. In each of the figures the temperature profiles at the middle of the plume are shown, one 300 m further away, and the last temperature profile 700 m away from the centre of the plume.

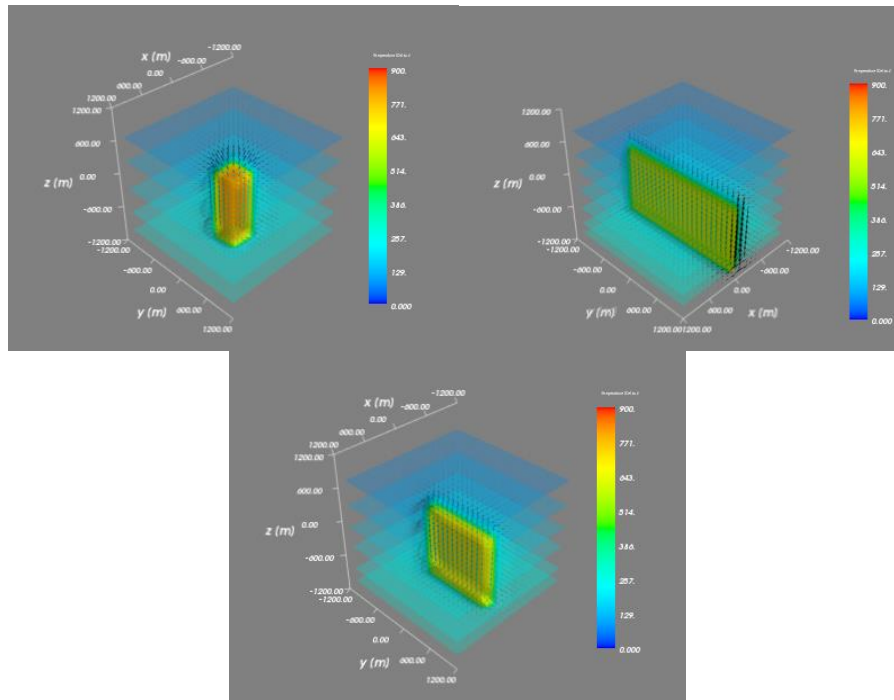


Figure 12. Temperature contours and total flow rate vectors for the intrusions after 200 years from start of simulation.

1.1.1.5.3 The long and narrow dike intrusion

In Figure 13 the case of the long dike intrusion is presented. This system can be considered to be a semi-2D system. On the temperature contour figure we see an emergence of a plume localised close to the original pluton injection. Also, in the temperature contour figure we see that two distinct convection cells on both sides of the intrusion. This is very typical of what we expect from a 2D simulation. The plume does not rise much and maintains a bell curve shape. In the temperature profiles we see a step appearing just below -1000 m depths but no inversion below the step.

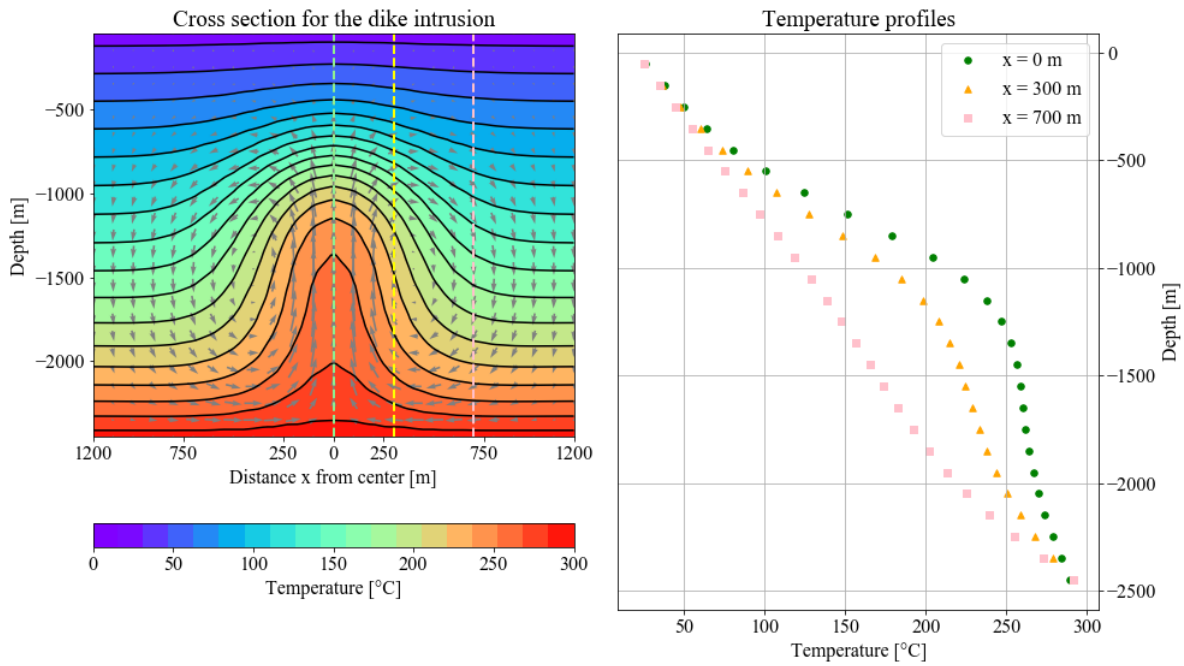


Figure 13. The system containing the narrow and long dike intrusion after 5000 years. On the left side are temperature contours for the cross section along the x axis and through the middle of the dike intrusion system. Also shown are fluid flow rate vectors in the cross section plane and the dashed lines indicate where the temperature profiles are taken. Temperature profiles taken at x=0 m, x=300 m and x=700 m are shown on the right.

1.1.1.5.4 The pillar intrusion

The case for the pillar intrusion after 5000 years is shown in Figure 14. For this case we see a plume that rises with large flow rate propelling it upward but no formation of distinct convection cells as was the case for the long and narrow dike. From temperature profiles we see a sign of temperature inversion at the centre of the plume.

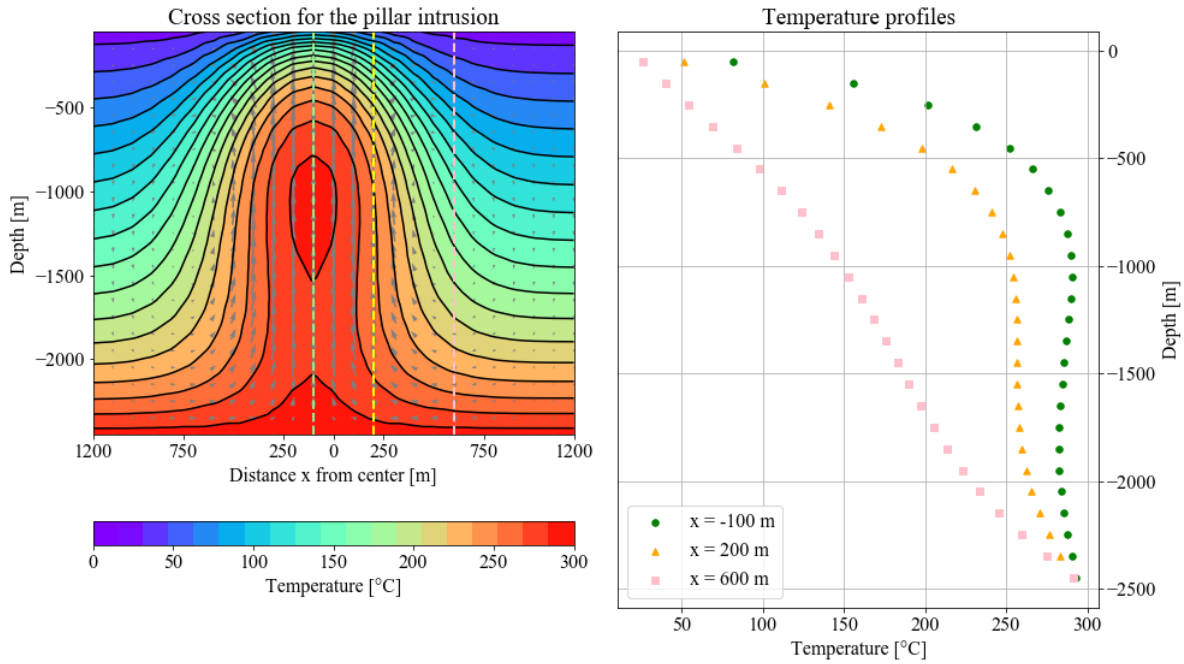


Figure 14. The system containing the pillar intrusion after 5000 years. On the left side are temperature contours for the cross section along the x axis and through the middle of the pillar intrusion system. Also shown are fluid flow rate vectors in the cross section plane and the dashed lines indicate where the temperature profiles are taken. To the right are temperature profiles taken at the centre of the intrusion $x = -100$ m, 200 m away from the centre of the intrusion and 700 m away.

1.1.1.5.5 The limited dike intrusion

The shape of limited dike is midway between the pillar system and the long dike system and is therefore a valuable case for comparison. The result for the limited dike system after 5000 years is shown in figure 15. It is interesting to see that it does show a plume and temperature profiles that are more in line with the what we see in the pillar intrusion than for the long dike intrusion; the main difference being that its temperature inversion is rather small. Although we see clearer sign of convection cells than for the pillar intrusion, the cells are not as clear and symmetric as for the long dike system.

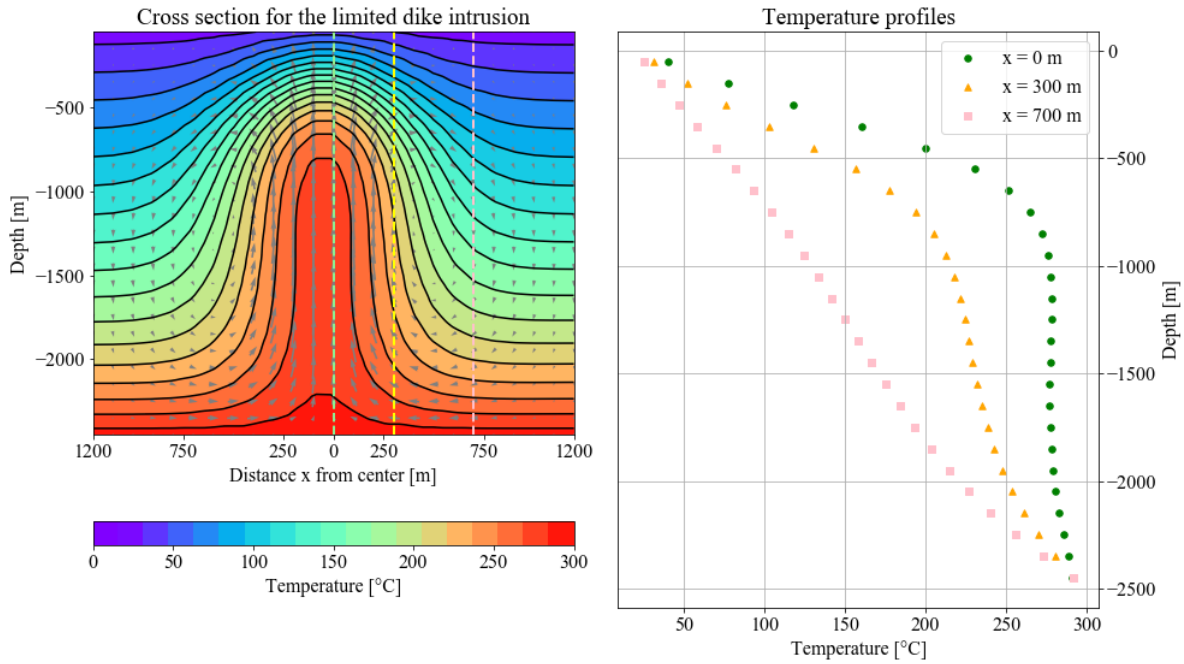


Figure 15. The system containing the limited dike intrusion after 5000 years. On the left side are temperature contours for the cross section along the x axis and through the middle of the dike intrusion system. Also shown are fluid flow rate vectors in the cross section plane and the dashed lines indicate where the temperature profiles are taken. To the right are temperature profiles taken at x=0 m, x=300 m and x=700 m.

1.1.1.5.6 Conclusions

For all three cases the long dike seems to stand out in two ways. First, its plume does not rise like in the other cases. This could be because it has a large surface to volume ratio and smaller top surface area than the other cases. This makes the long dike lose heat faster and warm the total system more evenly. The other feature that stands out is the clear and symmetric convection cells. This is probably due to the 2D nature of the system. For the long dike the flux area for the upstream and the downstream are closer in size than for the limited dike and pillar system. Also, because the system is completely uniform in the y direction there is negligible flow in the y direction which enhances convection cells that lie in the xz-plane.

1.1.1.6 Modelling of random magma intrusions with iTOUGH2 and EOS1sc

This case study involves a continuation of the work of Gunnarsson and Aradóttir (2014), using the tools developed in this project for high temperature and pressure, not available during the original work.

The model is 20 km long, 10 km wide and 3.4 km deep. Vertically, the model is divided into 17 layers. Layers close to the top are 100 m or 200 m thick; near the bottom, the layers are 300 m and 400 m thick. The top and bottom layers are inactive, and used as constant pressure and temperature boundaries. Thus, the active part of the model is 3 km thick. The elements are 230×230 m² at the centre of the model and 500×500 m² closer to the edges.

The reservoir is defined as the part of the model where the rock is permeable enough so that convection dominates the heat transfer. The reservoir is 9.9 km×3.2 km. The permeability in the reservoir is 15×10⁻¹⁵ m². A small area at the centre, has a higher permeability of 5×10⁻¹³ m². The reservoir is surrounded and capped by impermeable rocks. Outside the reservoir, the permeability is 10⁻¹⁸ m². Vertically, the permeable reservoir starts at -800 m and extends down to the bottom of the

active model at -3000 m. The permeability in the bottom layer and caprock (above -800 m) is 10^{-18} m^2 . In the reservoir, the porosity is 0.12, and in the impermeable rock outside the porosity is 0.01.

1.1.1.6.1 Heat sources and steady state

A common method to create natural-state, is to add heat source to the reservoir bottom layer, and run the model until a steady state is reached. In this example, heat sources were placed to entirely cover the reservoir bottom layer. The heat rates were scaled to provide a uniform heat rate per unit area. The heat rates were also adjusted to obtain a roughly uniform temperature of 300 °C, at the centre of the model. Figure 16 shows the temperature profile at different locations. Figure 17 shows the temperature horizontal distribution at -1050 m. The heat flux through the reservoir bottom layer (combining the heat from the model bottom layer and sources) is 35 MW, or 1.1 W m^{-2} .

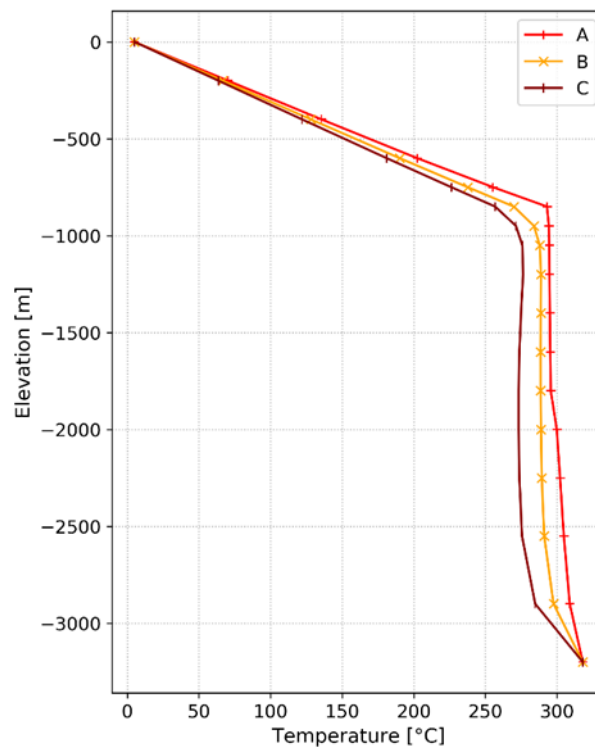


Figure 16. Temperature at location A, B, and C as indicated in the map in Figure 17.

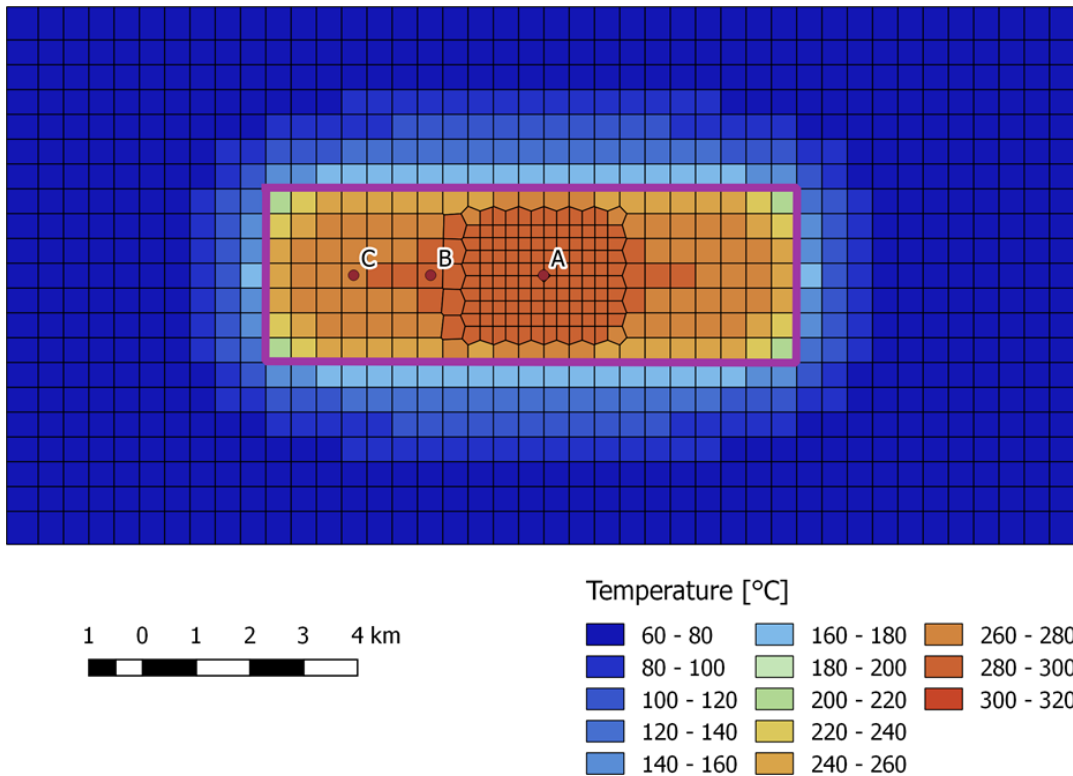


Figure 17. Mesh and temperature at -1050 m. Convection occurs inside the purple rectangle where the rock permeability is $15 \times 10^{-15} \text{ m}^2$. Outside the rectangle, where the permeability is 10^{-18} m^2 , heat is transferred by conduction. The model is $20 \text{ km} \times 10 \text{ km}$. The (purple rectangle) permeable area is $9.9 \text{ km} \times 3.2 \text{ km}$.

1.1.1.6.2 Random magma intrusions

The new equation of state module developed by Lilja Magnúsdóttir (see below), can simulate temperature up to a $1000 \text{ }^\circ\text{C}$. The module was used here and attempts were made to create a natural state by simulating intrusion of hot magma into the reservoir. This was performed by using command 'RESTART' in iTOUGH2 to reset the temperature and pressure of some randomly chosen elements at the bottom of the reservoir. All the intrusions have the same shape. They are made of vertically aligned elements in the three bottom layers at -3200 m , -2900 m , and -2550 m . The intrusions were simulated by resetting the selected elements' temperature to $800 \text{ }^\circ\text{C}$, and pressure to 75 MPa . The horizontal locations and times at which the resets occurred were chosen randomly. In its initial state, prior to the intrusion, the reservoir temperature is roughly $90 \text{ }^\circ\text{C}$.

100 intrusions in 10 000 years

The first scenario was set up to simulate a hundred intrusions in 10 000 years. Figure 18 shows the evolution of the temperature at the centre of the reservoir. After 2 000 years, the reservoir has warmed up to $170 \text{ }^\circ\text{C}$, and seems to have reached a steady state. During, the 8 000 remaining years of the simulation, the temperature fluctuates between $160 \text{ }^\circ\text{C}$ and $230 \text{ }^\circ\text{C}$.

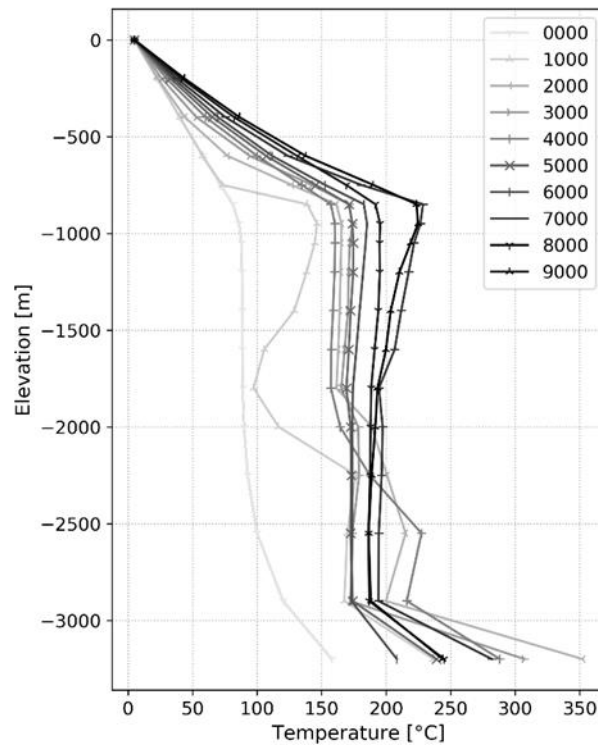


Figure 18. The figure shows temperature fluctuations at the centre of the reservoir, in the scenario where 100 years occur in 10,000 years.

200 intrusions in 10 000 years

The second scenario was set up to simulate 200 intrusions in 10,000 years. Figure 19 shows the temperature evolution at the centre of the reservoir. Around 7000 years are necessary to reach the temperature of around 300 °C. Figure 20 shows a map of the temperature at -1050 m, after 7 000 years. The result is like the one obtained by using constant head sources (Figure 17), but the model with intrusions has a less regular temperature distribution. Figure 21 shows the temperature at -2250 m after 7000 years.

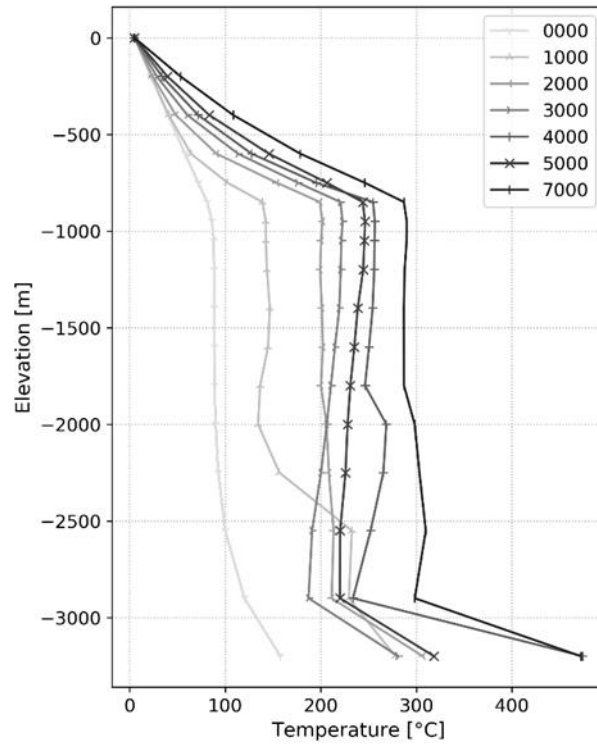


Figure 19. The figure shows the temperature evolution at the center of the reservoir, in the scenario where 200 intrusions occurs in 10,000 years.

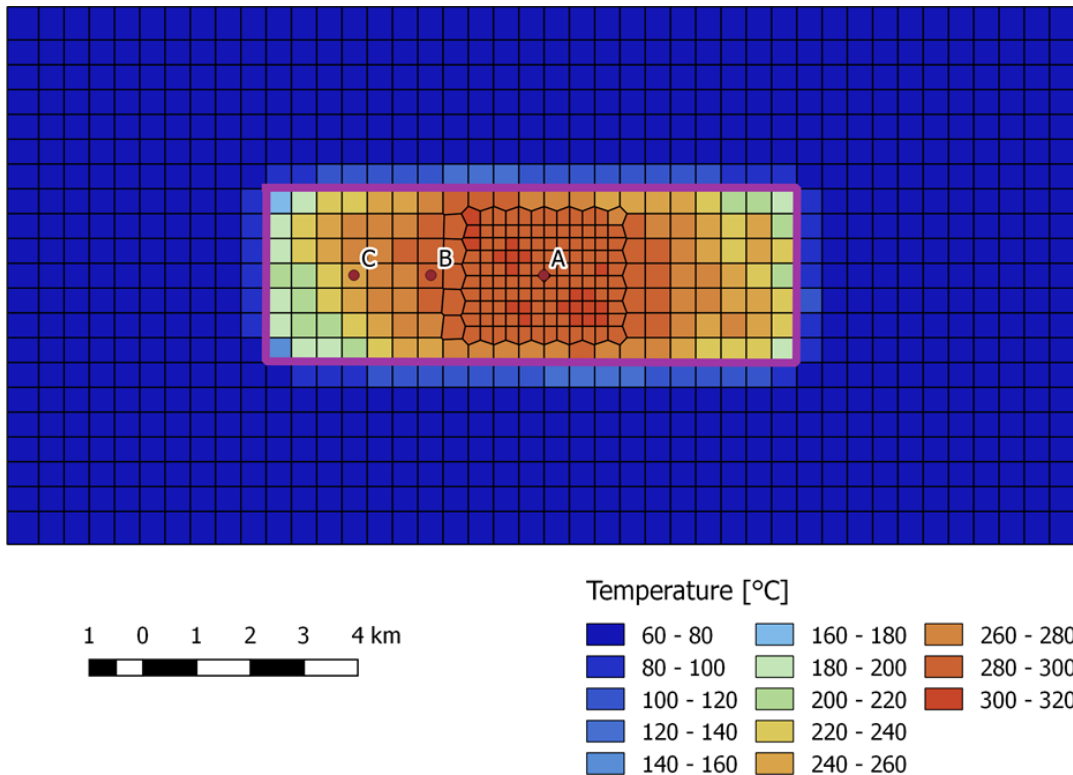


Figure 20. Temperature at -1050 m, after 7 000 years in the scenarios with 200 intrusions in 10,000 years.

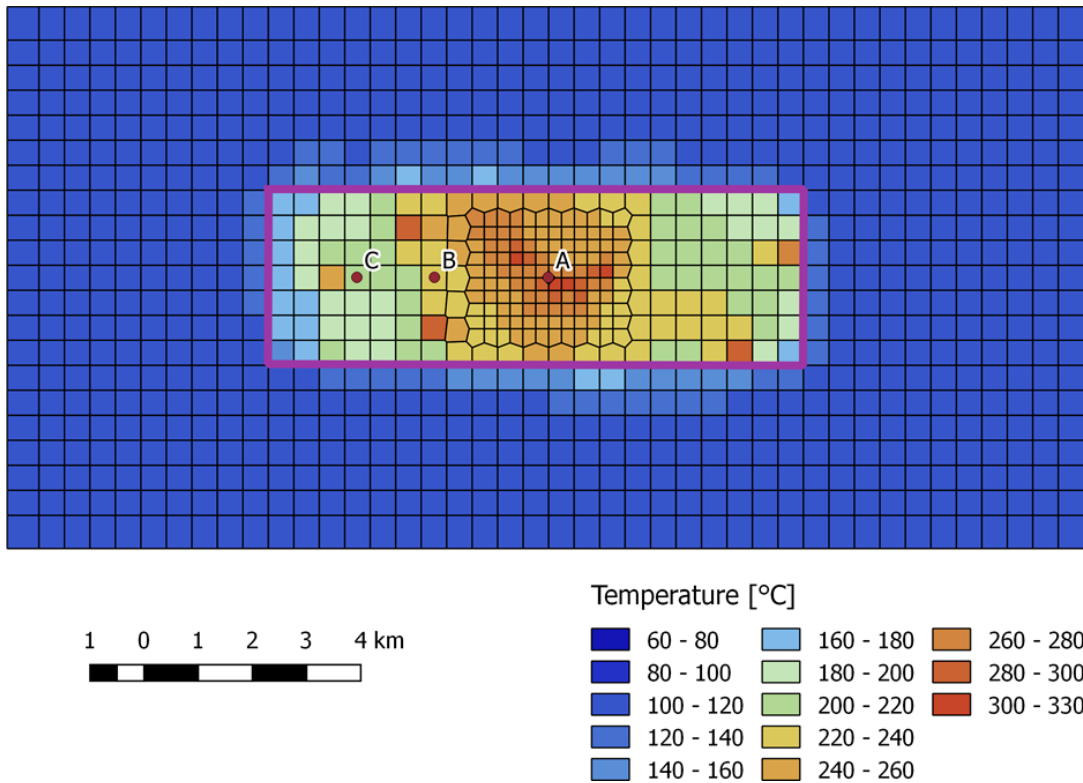


Figure 21. Temperature at -2250 m, after 7000 years in the scenarios with 200 intrusions in 10 000 years.

1.1.1.6.3 Conclusions

Natural states similar to the ones generated using constant sources, can be created by modeling the random intrusions of magma into the reservoir. However, the intrusion method resulted in a reservoir with a more irregular temperature distribution. The intrusion method also took significantly longer. With such a small model, generating a steady state takes using constant heat sources takes a few minutes. Modelling the water in supercritical conditions, the plutons and the complex convection patterns they induce required a few days to a couple of weeks.

1.1.2 Progress of Part 2.2

This sub-part of the project was undertaken by Lilja Magnúsdóttir, a postdoctoral fellow located in Berkeley, California, and coordinated by Gunnar Gunnarsson at Reykjavík Energy, with support from e.g. Stefan Finsterle at Lawrence Berkeley National Laboratory (LBNL) in Berkeley. The time schedule and progress for Part 2.2 of the DRG project, which was completed in 2015, is shown in Figure 28.

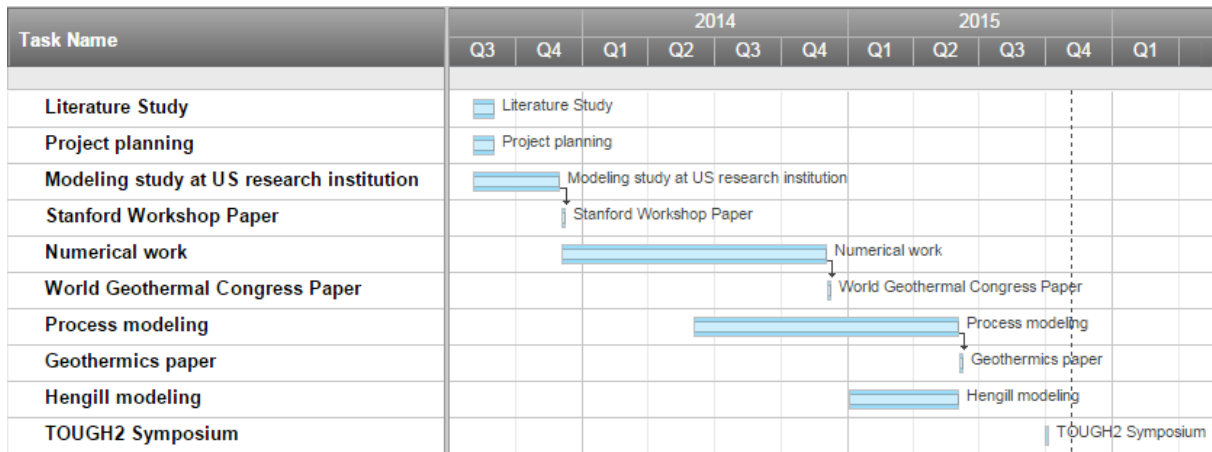


Figure 22: Time schedule and progress for Part 2.2 of the DRG project.

In December 2014, the numerical work of this project was completed. The last step of the numerical work was to further develop the new supercritical equation-of-state module EOS1sc (Magnusdottir and Finsterle, 2014) and to add an option to use temperature or depth dependent rock properties. That option allows the user to model various conditions present in magmatic geothermal reservoirs. For example, the brittle-ductile transition can be approximated by treating the permeability as a function of temperature, and heat capacity of a cooling intrusion can be increased to account for the latent heat of crystallization.

The temperature and depth dependent properties to be used in EOS1sc are specified in the TOUGH2 input file by defining IPFT in block ROCKS.4 for permeability, and ICFT in block ROCKS.5 for heat capacity, as follows:

ROCKS.4

IPFT = 1 Linear permeability changes
 2 Log-linear permeability changes

ROCKS.5

ICFT = 1 Linear heat capacity changes
 2 Log-linear heat capacity changes

For the process modeling work, a cooling pluton was modeled to demonstrate the forward and inverse capabilities of EOS1sc in iTOUGH2. The groundwater flow and heat transfer in the hydrothermal system was investigated as the pluton cools down and the results using iTOUGH2 were compared to results using HYDROTHERM. Inverse analysis was then used to estimate the initial temperature of the pluton and the permeability of the geothermal reservoir by using observations of injection pressure, production temperature, and production rate after the reservoir had reached steady-state.

The model is two-dimensional with dimensions $4 \times 10 \text{ km}^2$ and a nominal thickness of 1 m. A pluton with dimensions $0.5 \times 1.5 \text{ km}^2$ was emplaced at a depth of 2.5 km. The basaltic rock consists of four regions and the surface temperature and pressure were set constant at 20°C and 1 atm. A temperature gradient of $100^\circ\text{C}/\text{km}$ and hydrostatic pressure were modelled. The initial temperature of the pluton was set as $1,100^\circ\text{C}$, thus assuming that there is a heat source beneath from which the pluton intruded.

First, the forward problem was studied of the pluton cooling down until the reservoir reaches steady state. The temperature distribution 5,000 years after the magma intrusion is shown in Figure 29. The geothermal system is highly permeable ($k = 10^{-14} \text{ m}^2$) which results in heat transfer dominated by advection. The density-driven fluid migration is rapid and an upwelling plume with temperatures higher than 250°C forms directly above the cooling pluton.

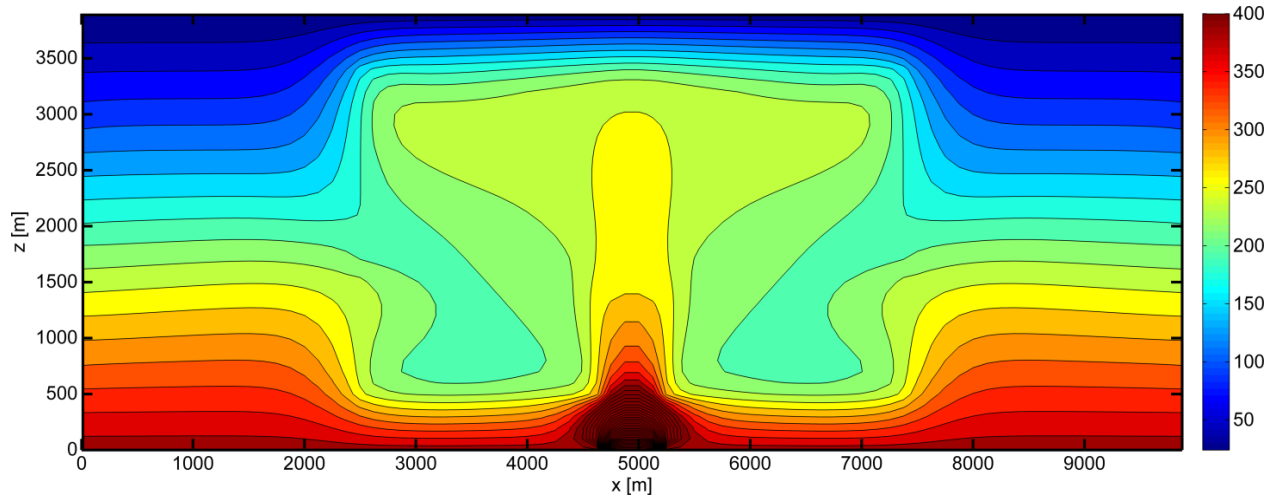


Figure 23: Temperature distribution (°C) at 5,000 years after the intrusion. The maximum temperature at elements below the intrusion is 1,100°C.

Next, an inversion of synthetically generated exploitation data was performed to demonstrate an iTOUGH2 application in combination with the new EOS1sc module.

Fluid with an enthalpy of 500 kJ/kg was injected at a constant rate and the injection pressure was monitored. Temperature and extraction rates were observed in a production well located above the intrusion. Then, the pressure, temperature, and production-rate data were corrupted by Gaussian noise with standard deviations of 2 bars, 3 °C, and 0.1 kg/s, respectively. Data was collected monthly during the first 5 years of production and then the calibrated model was used to predict reservoir performance for an additional 15 years.

For this demonstration, the logarithm of reservoir permeability and initial pluton temperature were considered the unknown parameters to be estimated by history matching. Since the initial pluton temperature was updated during the inversion, a natural-state calculation starting from the time of the intrusion was needed, followed by a simulation of the transient behaviour during reservoir exploitation.

The parameters were estimated by solving a non-linear weighted least-squares problem using five iterations of the Levenberg-Marquardt minimization algorithm. Estimation and prediction uncertainties were approximately calculated assuming the model is linear within the confidence region and the errors are normally distributed.

Figure 30 shows the true system behaviour, the noisy synthetic observations used as calibration points during the first five years of production, the long-term system behaviour, and the corresponding model predictions with the initial (i.e., uncalibrated) and calibrated models. It is obvious that even relatively minor errors in the two parameters examined here lead to grossly different predictions of reservoir behaviour; a calibration step is thus essential. iTOUGH2 is capable of

identifying the true parameter set within a few iterations, thus matching the calibration data and yielding a reasonable prediction of future reservoir behaviour, specifically the considerable long-term temperature decline in the production well despite the near-by presence of a hot pluton.

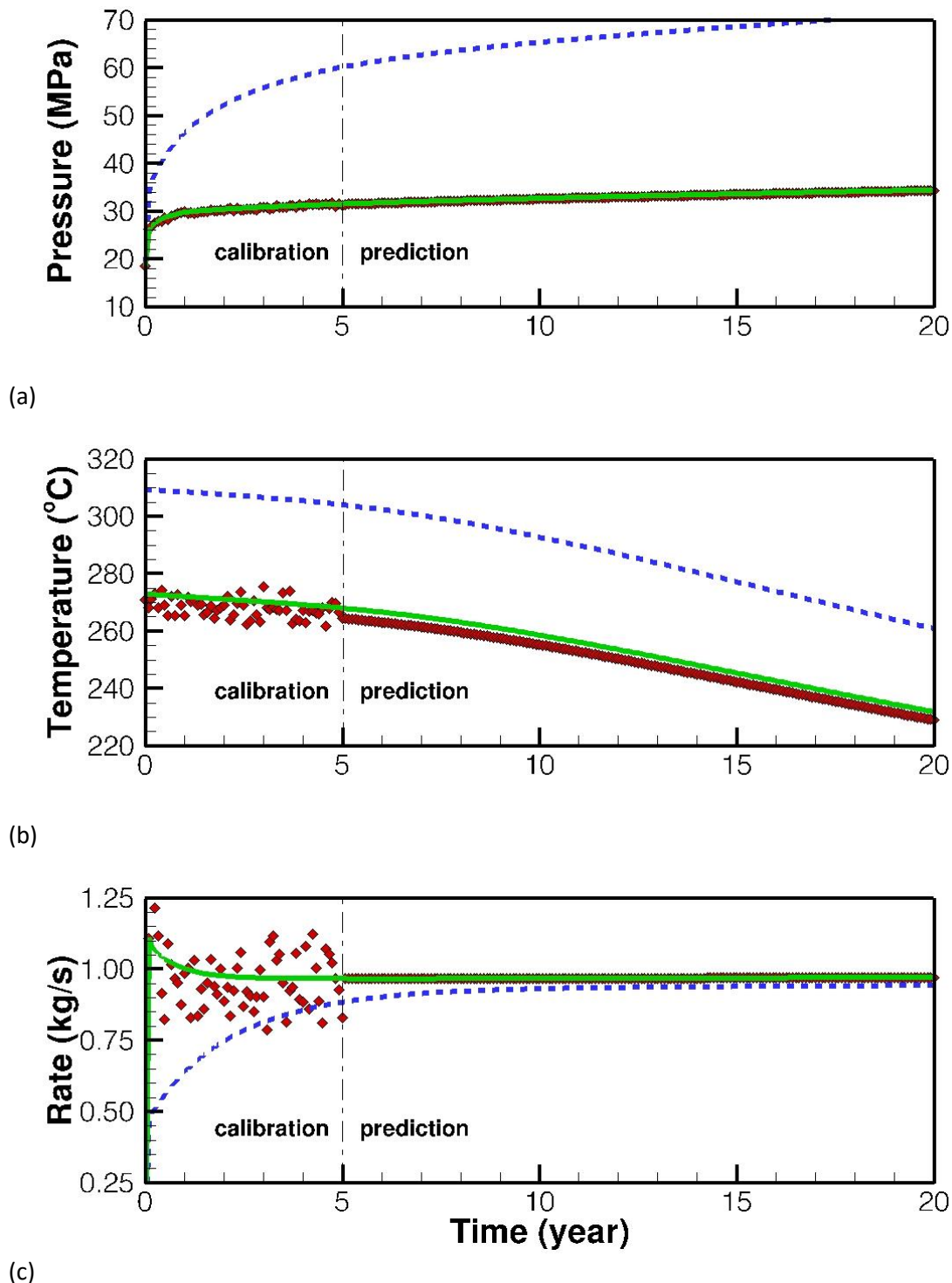


Figure 24: (a) Injection pressure, (b) production temperature, and (c) production rates simulated with the uncalibrated model (dashed lines), and calibrated model (solid lines); the synthetic data used for model calibration during the first five years of production are shown as symbols.

This generic data inversion and associated analyses demonstrate that the newly developed equation-of-state module for sub- and supercritical water was successfully integrated into the iTOUGH2 simulation-inversion framework. It also indicates that simulating the deep heat source is essential, as it influences reservoir performance and the estimation of parameters that are correlated to the properties and conditions of, for example, an intrusion. A more detailed description of this study as well as a comparison of using HYDROTHERM instead of EOS1sc in iTOUGH2, were published in GEOTHERMICS (Magnusdottir and Finsterle, 2015b).

Part 2.2 of the DRG project progressed according to the schedule except that the end date was changed from August 2015 to the end of May 2015. The final step of Part 2.2 included developing a model of the Hengill geothermal reservoir in Iceland based on a model provided by Gunnar Gunnarsson at Reykjavik Energy. The model was updated to make it compatible with recent versions of iTOUGH2 so it could be simulated using EOS1sc. Also, instead of injecting heat close to the bottom boundary of the model, the depth of the model was increased and some part of the rock was modeled at supercritical temperatures to account for intrusions. Inverse files for the forward model were prepared as well where the initial temperature of the intrusions and the permeability of the reservoir can be evaluated based on production data.

In 2015, Lilja Magnusdottir presented her work at the World Geothermal Congress 2015 in Melbourne, Australia and at the TOUGH2 Symposium 2015 in Berkeley, USA.

After Lilja's involvement in this GEORG-project ended, she did continue intermittently improving the EOS1sc. The status of this will be presented (paper + presentation) at the Stanford Geothermal Workshop 2018 in February next year. The associated abstract states:

“A numerical simulator capable of modeling supercritical conditions in geothermal reservoirs is crucial for better understanding the deep roots of geothermal systems. This paper describes improvements made to the EOS1sc module in iTOUGH2 for increasing the reliability of the supercritical module. Some discontinuities are present in thermodynamic properties covering the four regions of the thermodynamic formulation used; liquid, steam, supercritical, and two-phase. Although these discontinuities are relatively small, they can cause convergence issues especially for complex supercritical flow problems. In order to eliminate discontinuities across boundaries of the thermodynamic regions, cubic Bezier curves were implemented into the EOS1sc module for interpolating between two thermodynamic regions. By using Bezier curves instead of linear interpolation, sharp corners and related convergence issues were avoided. In addition, new backward equations for specific volume as a function of pressure and temperature were implemented in the supercritical region to increase the reliability of the EOS1sc module as well as the speed. The new formulation is approximately seven times faster than the Newton-Raphson method that was previously used to iteratively calculate the density in that region. Thereby, by implementing new backward equations and cubic Bezier curves, poor convergence at intersection points between thermodynamic regions were resolved and the speed as well as reliability of the supercritical EOS1sc module was increased.”

References

Magnusdottir, L., and Finsterle, S.: Extending the Applicability of the iTOUGH2 Simulator to Supercritical Conditions, World Geothermal Congress 2015, Melbourne, Australia, (2015a).

Magnusdottir, L., and S. Finsterle: *An iTOUGH2 equation-of-state module for modeling supercritical conditions in geothermal reservoirs, Geothermics, 57, 8–17, (2015b).*

Magnusdottir, L., and Finsterle, S.: *iTOUGH2-EOS1sc: Multiphase Reservoir Simulator for Water under Sub- and Supercritical Conditions, User's Guide, Lawrence Berkeley National Laboratory, (2014).*

1.1.3 Other work

In addition to the work carried out by the three reservoir modelling specialists the following was accomplished in connection with Part 2 of the DRG-project:

- A poster-presentation on the DRG-project at the information booth of the IES Geothermal Implementing Agreement at the WGC2015, April 19 – 24, by Gudni Axelsson *et al.* at ÍSOR (see Appendix)

Finally links with the IPGT cooperation (<http://internationalgeothermal.org/index.html>), the COTHERM project, financed by the Swiss Government, and the International Energy Agency's Geothermal Implementing Agreement, should be noted. Informal discussions with participants of these activities have taken place at various meeting in Iceland and internationally.

1.2 Schedule modification

The project schedule has been modified somewhat during the 4-year course of the project. One principal change involved increasing initially the emphasis on Part 2.2, with the aim of completing that task in a little over 2 years, while reducing the emphasis on Part 2.1 initially, which consequently started out more slowly than originally planned. Another principal change involved less interaction with ETH during the later stages of the project than planned. The need for such interaction turned out to be less than originally planned, partly because of the success of part 2.2 of the project, and other related changes regarding the iTOUGH2-code (temperature-dependent permeability as in Hydrotherm and CSMP++). In addition, some minor modifications were made to details of the schedule, based on issues encountered during the progress of the project, are mentioned above.

1.3 Summarized main results

The overall results of the modelling group, which mainly carried out the DRG Part 2 project, were quite satisfactory. The capabilities of the major candidate simulators for supercritical fluid (Hydrotherm and CSMP++) were thoroughly investigated. In addition, the most commonly used simulation package in the geothermal industry, TOUGH2 and iTOUGH2, was successfully extended to be able to handle supercritical fluid. Finally, two peer reviewed publications and three conference papers were published.

The main achievements and results of the whole project may be listed as follows:

- Comprehensive training in the use of Hydrotherm and CSMP++.
- These software applied to various hypothetical models (case studies), relevant for increased understanding of geothermal activity around intrusions. Including IDDP-1 case study.
- Neither Hydrotherm nor CSMP++ appear suitable for industry-style modelling, but are valuable for more academic modelling.
- New EOS for TOUGH2/iTOUGH2 (EOS1sc) developed within the project. It is extremely valuable, extends applicability of software to much higher p+T and greater depth (has been limiting, e.g. for the Krafla system).

- Temperature dependent rock permeability has been incorporated in TOUGH2/iTOUGH2, yet outside the GEORG project. Makes the software even more versatile and makes it resemble Hydrotherm and CSMP++ in deep-root applicability.
- TOUGH2/iTOUGH2 with new capabilities applied to further theoretical case-studies (intrusions of various shapes and sizes).
- TOUGH2/iTOUGH2 with new capabilities applied Krafla related case studies, including studies of IDDP-1.
- TOUGH2/iTOUGH2 with new capabilities applied to random dike-injection (heat sources) model.
- Modification of existing Hengill numerical model performed in preparation of applying new capabilities of TOUGH2/iTOUGH2.
- Industry will greatly benefit from both increased understanding and improved modelling tools.

2 Project Management

The finances and work plan outlined in the grant submission document frame the project. Given the qualifications of the reservoir modelling experts, all detailed planning on how to carry out the modelling work was left to them with very satisfactory results. Based on their suggestions, some of the project tasks were revised as discussed in section 1.2. A number of project meetings were held, both for each of the project parts (2.1 and 2.2), as well as for the project as a whole.

3 Student involvement

No students were involved in Part 2 of the DRG project.

4 Publications and disseminations

The following publications have been produced as part of the project:

Magnusdottir, L., and S. Finsterle, 2015: An iTOUGH2 equation-of-state module for modeling supercritical conditions in geothermal reservoirs, *Geothermics*, **57**, 8–17.

Magnusdottir, L., and S. Finsterle, 2015: Simulating Supercritical Water in Magmatic Geothermal Reservoirs, *PROCEEDINGS, TOUGH Symposium 2015*, Lawrence Berkeley National Laboratory, Berkeley, California.

Magnusdottir, L., 2014: Modeling the Deep Roots of Geothermal Systems, *PROCEEDINGS, Thirty-Ninth Workshop on Geothermal Reservoir Engineering*, Stanford University, Stanford, California, 11 pp.

Magnusdottir, L., and S. Finsterle, 2015: Extending the Applicability of the iTOUGH2 Simulator to Supercritical Conditions, *PROCEEDINGS, World Geothermal Congress 2015*, Melbourne, Australia, 8 pp.

Gunnarsson, G., and E.S.P. Aradóttir, 2014: The Deep roots of geothermal systems in volcanic areas: Boundary conditions and heat sources in reservoir modelling. *Transport in Porous Media*, published online May 23, 2014, 17 pp., DOI 10.1007/s11242-014-0328-1.

Axelsson, G., K. Árnason, H. Franzson, G. Gunnarsson, S. Hreinsdóttir, E. Júlíusson, 2014: The roots of volcanic geothermal systems. Poster and abstract at Deep Geothermal Days, April 10 – 11, Paris.

In addition Part 2 of the DRG project has been introduced/presented at different functions worldwide as well as in Iceland, some of these occasions are mentioned above.

Part 2 of the DRG project was, of course, heavily represented at the DRG Conference in Reykjavik, February 18 – 19, 2016, see <http://georg.cluster.is/events-georg/>.

Finally, Part 2 of the DRG project will be presented at the Stanford Geothermal Workshop in February 2018 through the following two papers/presentations:

Magnusdottir, L., and M.Th. Jonsson, 2018: Increased reliability of supercritical EOS1sc module in iTOUGH2.

Thorgilsson, G., Axelsson, G., Berthet, J.C.C., Magnusdottir, L., Árnason, K., Gunnarsson, G., and Júlíusson, E., 2018: Modelling of the Deep Roots of Volcanic Geothermal Systems.

5 Cost statement

The budget plan for Part 2 of the DRG-project and the real cost for the duration of the project are presented in Table 2 below. The real salary cost for the post-doctorate is nearly the same as planned while the salary cost for the two ÍSOR and Vatnaskil modelling specialists is considerably higher than planned. This also applies to the advisory contribution by ÍSOR. In contrast, the actual work-input from the advisory group of the other participants (HÍ, LV, OR and HS-Orka) turned out to be less than planned.

Travel costs turned out to be about 2/3 of what was originally planned, mainly because the second study-trip to ETH in Switzerland was cancelled. It was deemed to be not necessary because of the improvements made in the iTOUGH2 platform.

Table 2: The budget plan for Part 2 of the DRG-project and real cost for the duration of the project.

Consortium: Part 2		Budget plan															
PI: Guðni Axelsson/Robert K. Podgorney																	
Financial Manager: Guðni Axelsson																	
Name of Project: Deep roots of geothermal systems																	
ISK '000	Year	Unit cost	Year 1				Year 2				Year 3				Total		
			Man-months	Total	Man-months	Total	Man-months	Total	Man-months	Total	Man-months	Total	Man-months	Total	GEORG	Co-financing	Grand tot
Salaries including overhead																	
Ph.D. student	NN	350	0,0	0	0	0,0	0	0	0,0	0	0	0,0	0	0	0	0	0
Modeling specialist	NN	650	6,0	3.900	0	6,0	3.900	0	6,0	3.900	0	6,0	3.900	0	11.700	0	11.700
Post doctorate	LM	500	12,0	6.000	0	12,0	6.000	0	6,0	3.000	0	6,0	3.000	0	15.000	0	15.000
Advisor	GAX	1.000	0	0,5	500	0	0,5	500	0	1,0	1.000	0	1,0	1.000	0	2.000	2.000
Advisor	HP	1.000	0	1,0	1.000	0	1,0	1.000	0	2,0	2.000	0	2,0	2.000	0	4.000	4.000
Advisor	GG	1.000	0	1,0	1.000	0	1,0	1.000	0	2,0	2.000	0	2,0	2.000	0	4.000	4.000
Advisor	EJ	1.000	0	1,0	1.000	0	1,0	1.000	0	2,0	2.000	0	2,0	2.000	0	4.000	4.000
Advisor	ÓS	1.000	0	0,5	500	0	0,5	500	0	1,0	1.000	0	1,0	1.000	0	2.000	2.000
Salaries Total			18	9.900	4	4.000	18	9.900	4	4.000	12	6.900	8	8.000	26.700	16.000	42.700
Computer for model calculations			350												350	0	350
Operation Total			350		0		0		0		0		0		350	0	350
Post doctorate			500			500			500					1.500		1.500	
Modeling specialist			500			500			500					1.500		1.500	
Travel Total			1.000		0	1.000		0	1.000		0		3.000		3.000		3.000
Total			11.250		4.000	10.900		4.000	7.900		8.000		30.050	16.000	46.050		

Consortium: Part 2		Real cost															
PI: Robert K. Podgorney																	
Financial Manager: Guðni Axelsson																	
Name of Project: Deep roots of geothermal systems																	
ISK '000	Year	Unit cost	Year 1				Year 2				Year 3				Total		
			Man-months	Total	Man-months	Total	Man-months	Total	Man-months	Total	Man-months	Total	Man-months	Total	GEORG	Co-financing	Grand tot
Salaries including overhead																	
Ph.D. student	NN	350	0	0	0	0	0	0	0	0	0	0	0	0	0	0	0
Modeling specialist	GP/JCCB	750	4,7	3.525	0	6,2	4.650	0	6,5	4.875	3,4	2.550	13,050	2.550	15.600		15.600
Post doctorate	LM	650	11,0	7.150	0	12,0	7.800	0	0	0	0	0	14.950	0	14.950		14.950
Advisor	GAX/KÁ	1.100	0	0,8	880	0	1,2	1.320	0	1,3	1.430	0	3,630	3.630	3.630		3.630
Advisor	HP	1.000	0	0,1	100	0	0,1	100	0	0	0	0	200	200	200		200
Advisor	GG	1.100	0	1,0	1.100	0	1,2	1.320	0	1,3	1.430	0	3.850	3.850	3.850		3.850
Advisor	EJ	1.100	0	0,3	330	0	0,5	550	0	0,8	880	0	1.760	1.760	1.760		1.760
Advisor	ÓS	1.100	0	0,1	110	0	0,1	110	0	0	0	0	220	220	220		220
Salaries Total			16	10.675	2	2.520	18	12.450	3	3.400	7	4.875	7	6.290	28.000	12.210	40.210
Computer for model calculations			0		0		0		0		0		0	0	0	0	0
Operation Total			0		0		0		0		0		0	0	0	0	0
Post doctorate			562			699			1.261				1.261		1.261		1.261
Modeling specialist			745			0			745				745		745		745
Travel Total			1.307		0	699		0	0		0		2.006		2.006		2.006
Total			11.982		2.520	13.149		3.400	4.875		6.290		30.006	12.210	42.216		

Appendix - Relevant Publications